

Research papers

Deciphering large-scale spatial pattern and modulators of dissolved greenhouse gases (CO₂, CH₄, and N₂O) along the Yangtze River, China

Peifang Leng^{a,b}, Zhao Li^a, Qiuying Zhang^{c,*}, Matthias Koschorreck^b, Fadong Li^{a,d}, Yunfeng Qiao^{a,d}, Jun Xia^e

^a Key Laboratory of Ecosystem Network Observation and Modeling, Institute of Geographic Sciences and Natural Resources Research, Chinese Academy of Sciences, 100101 Beijing, China

^b Department of Lake Research, Helmholtz Centre for Environmental Research-UFZ, 39114 Magdeburg, Germany

^c Chinese Research Academy of Environmental Sciences, 100012 Beijing, China

^d College of Resources and Environment, University of Chinese Academy of Sciences, 100190 Beijing, China

^e State Key Laboratory of Water Resources & Hydropower Engineering Sciences, Wuhan University, Wuhan 430072, China

ARTICLE INFO

Handling Editor: Dr N. Basu

Keywords:

Greenhouse gases
Yangtze River
Dissolved concentrations
Spatial pattern
Wetland
Oxygen

ABSTRACT

The Yangtze River, the third largest river around the globe, has been heavily engineered with a series of hydroelectric dams. Meanwhile, it receives elevated organic matter and nutrient loads from its densely populated catchment, subsequently altering dissolved greenhouse gas (GHG) concentrations along the river. However, the large-scale longitudinal patterns and drivers of GHG concentrations in the Yangtze River remain poorly understood. Using longitudinal sampling design in a 2400 km section, we report dissolved carbon dioxide, methane, and nitrous oxide concentrations along the Yangtze River at 145 sites. We observe significant spatial clustering with higher carbon dioxide and nitrous oxide concentrations in the middle reach of the Yangtze River. The results of nonlinear regression reveal that riverine GHGs are high when wetland coverage is high and dissolved oxygen is low. Wetlands and oxygen, not the Three Gorges Dam and tributaries, are the primary correlates of spatial variations of CO₂ and CH₄ concentrations, respectively. N₂O is surprisingly well predicted by CO₂, implying their common drivers or sources. We strongly recommend that wetland contribution to GHG budgets and its sensitivity to environmental change be considered when estimating riverine GHGs in the Yangtze River. In light of our study, future control of GHG emissions from large rivers may largely depend on how external inputs and internal metabolism are regulated by decreasing nutrient loading.

1. Introduction

Rivers are important players in the global budgets of long-lived greenhouse gases (GHGs), acting as an active pipe responsible for a disproportionately large amount of carbon and nitrogen processing, emission, and export from land to ocean (Bernhardt et al., 2022; Cole et al., 2007; Kroeze et al., 2005; Stanley et al., 2022). It is estimated that aquatic carbon can offset 12–590% of the terrestrial net ecosystem productivity among different types of ecosystems (Webb et al., 2019). Global rivers are estimated to produce 0.18%–0.28% of the emitted N₂O globally (Maavara et al., 2019) with higher N₂O emission fluxes in temperate and subtropical rivers (Hu et al., 2016). Omitting aquatic components in large scale GHG budgets may overestimate the magnitude of carbon and nitrogen storage in terrestrial ecosystems (Beaulieu

et al., 2011; Crawford et al., 2014); however, the estimates of GHG emissions from rivers are extremely uncertain due to the highly skewed spatial distributions of the river datasets (Liu et al., 2022; Maavara et al., 2019; Stanley et al., 2022).

Large rivers in (sub)tropical regions are recognized as important contributors of GHGs due to large surface area and higher rate of emissions per unit area compared to temperate ecosystems (Borges et al., 2015b; Hu et al., 2016; Raymond et al., 2013). These large rivers are, however, still under-represented in global datasets, particularly with respect to direct measurements of concentrations and fluxes (Borges et al., 2015a; Raymond et al., 2013; Regnier et al., 2013). Rivers in agricultural and urban area generally have higher GHG emissions (Beaulieu et al., 2011; Borges et al., 2018; Hu et al., 2016; Wang et al., 2017). Given the great importance of (sub)tropical rivers in the global

* Corresponding author.

E-mail address: zhangqy@craes.org.cn (Q. Zhang).

<https://doi.org/10.1016/j.jhydrol.2023.129710>

Received 8 July 2022; Received in revised form 16 April 2023; Accepted 19 May 2023

Available online 23 May 2023

0022-1694/© 2023 Elsevier B.V. All rights reserved.

river surface area, these rivers are presumably vital in the global GHG budgets, but the origins and controls over the fate of these GHGs are still poorly understood.

The paucity of available data, coupled with poor ecological understanding of the underlying processes, precludes us from predicting GHG spatial variability across the large river scale (Bussmann et al., 2022; Crawford et al., 2017a). Active gas transfer, low solubility, and elusive origins are responsible for the uncertainty of GHG concentrations and emissions from river networks (Marzadri et al., 2021; Stanley et al., 2016). Identifying the role of large rivers in regional and global GHG budgets necessitates an understanding of the linkages between riverine GHGs and catchment characteristics, since the rivers are fueled by C production and stocks from upland terrestrial and wetland (Borges et al., 2015b; Hotchkiss et al., 2015), in particular given that approximately half of the global surface area of wetlands is located in the (sub)tropics (Rivera-Monroy et al., 2011). Mobilized nutrients and organic matter potentially enhance the breakdown of terrestrially-derived organic carbon (OC) by heterotrophic river microbes (Ward et al., 2016). Meanwhile, in a highly disturbed large river, gross primary production (GPP) may exceed aerobic respiration, leading to CO₂ deficient

(Crawford et al., 2016). CH₄ is considered to be modulated by different biophysical controls than CO₂ (Rovelli et al., 2022). Although it is clear that excess N inputs from fertilizer and wastewater treatment plants clearly prompted N₂O concentrations, the controls of the biogeochemical processes producing N₂O in lotic systems are still not well understood.

In this study, we selected the Yangtze River to investigate the large-scale spatial patterns of dissolved GHGs along the river. The Yangtze River is the world's largest subtropical river confronting intensive human activities during recent decades. It has received widespread attention with respect to GHGs in Three Gorges Dam (TGD) at various spatial and temporal scales (Zhang et al., 2020; Zhao et al., 2013) and fluvial carbon export from the estuary (Wu et al., 2007; Zhang et al., 2008). Yet studies that addressed how hydrological and biological controls shift through the length of the Yangtze River with consequences of GHG variations are lacking. The river, which flows from the Tibetan Plateau into the sea, is characterized by a large gradient in hydro-morphological and biogeochemical configuration, which provides an ideal system to disentangle the mechanisms regulating large-scale patterns. Accordingly, we asked: what are the patterns and controls of

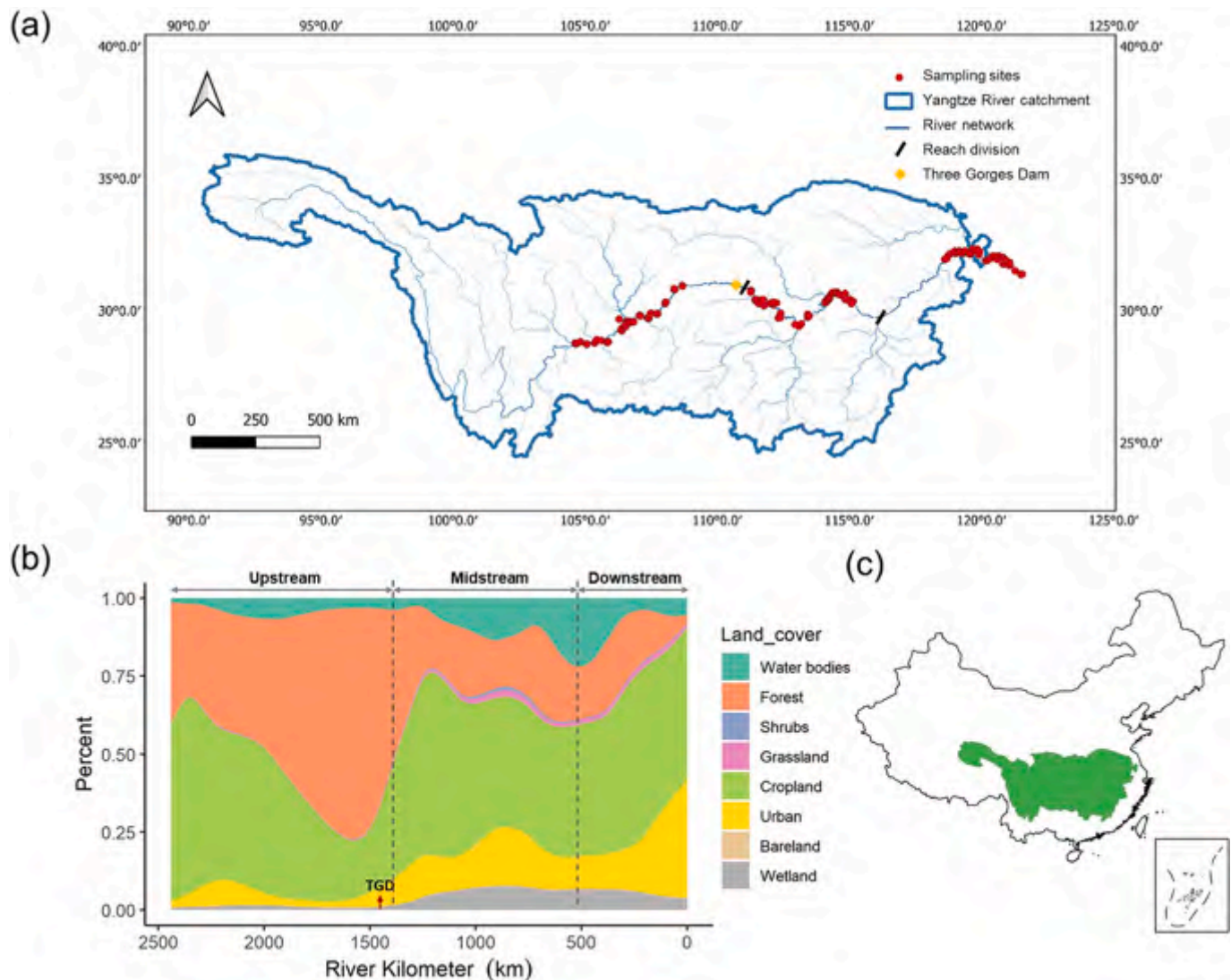


Fig. 1. (a) The Yangtze River system with sampling sites ($n = 145$) located in the upstream reach, midstream reach, and downstream reach, respectively. The blue lines with different shades represent the river network within the Yangtze River Catchment. (b) The percentages of different land covers along the Yangtze River. The river kilometer represents the river length from the estuary. When river kilometer is zero, it is the outlet of the Yangtze River Catchment. The land cover information is derived from the Copernicus Global Land Service from 2019. Red arrow refers to the location of the Three Gorges Dam (TGD). (c) The relative location of the Yangtze River Basin in China. (For interpretation of the references to colour in this figure legend, the reader is referred to the web version of this article.)

dissolved GHGs throughout the Yangtze River? To answer this, we conducted a sampling campaign in the Yangtze River to collect measurements of GHG concentrations and supporting water chemistry parameters, and integrated the results with hydromorphological attributes across the upper, middle, and lower reaches. We address our question by (1) generating a spatial dataset of dissolved GHG concentrations, (2) examining the relationships between GHG concentrations and potential drivers to understand and predict spatial trends of GHGs, and (3) gaining insights into the role of different sources of GHGs at the large-river scale.

2. Material and methods

2.1. Study area and sampling overview

The Yangtze (Changjiang) River Basin is located in a subtropical zone with an average annual precipitation of 1100 mm. Precipitation between May and October accounts for 70–90% of the annual total. The Yangtze River is a large river that rises in the Qinghai-Tibetan plateau and flows through the Sichuan Basin, the Three Gorges Reservoir, and the Middle-Lower Yangtze Plains into the East China Sea (total length 6300 km, catchment area $\sim 1.8 \times 10^6$ km², average annual discharge 960 km³ yr⁻¹ entering the sea). According to the topographic settings, the mainstem of the Yangtze River can be divided into three reaches: the reach upstream of Yichang, the reach between Yichang and Hukou, and the reach downstream of Hukou flowing through the low-gradient Yangtze Plain (Fig. 1a). The catchment is densely populated and the river serves as the water resource for one-third of China's population. Throughout the catchment, there is a conversion of land cover from forest to urban and grassland (Fig. 1b). Major city clusters along water courses are Chongqing, Wuhan, and Nanjing, which are located in the upstream, midstream, and downstream of the Yangtze River, respectively. Fluvial export of water, sediment, carbon, and dissolved solutes has been affected by human disturbance and climate change. The discharge of Yangtze River is monitored at 13 gauging stations by the Yangtze River Conservancy Commission, Ministry of Water Resources, China. Water discharge of large tributaries flowing into the Yangtze River was also monitored at gauging stations.

Our study was conducted in the mainstem and tributaries of the Yangtze River. The samples were taken downstream from October 17th to November 4th 2020 using a synoptic survey approach in which geomorphological characteristics, land cover information, and water physical and chemical parameters were acquired. 145 samples were selected from the upper, middle, and lower reaches of Yangtze River Basin with 76 sites from the mainstem and 69 sites from tributaries. The sampling locations were mainly accessed by bridges and boats, otherwise by the shore in the situation of no bridge and cruise. To examine the effect of tributaries, the sample sites were assigned at the outlets of tributaries and up- and downstream in the mainstem. The downstream sampling sites were located where tributaries and mainstem were well mixed.

2.2. Water chemistry and gas concentration analysis

In situ water temperature, specific conductivity, pH, and dissolved oxygen were determined using a multi-parameter portable meter (Hach H40d, USA). Water samples were collected in duplicate and filtered on site using 0.45 μ m filters in 50 mL polypropylene bottles for laboratory measurement. Samples for nitrate (NO₃⁻), ammonium (NH₄⁺), and dissolved total phosphorus (DTP) concentrations were stored at 4 °C for later lab analysis. Alkalinity was determined by titrating 50 mL filtered water with 0.01 M H₂SO₄ solution after sampling at a precision of 6% within 24 h. NO₃⁻ and NH₄⁺ were determined using the ion chromatography method (Dionex ICS 900; Dionex, USA) and the automated phenate method, respectively. Calibration curves were produced using reference samples according to quality control standards and were then applied to evaluate data from each set of samples. Reagents, procedural

blanks, and samples were measured twice in parallel, with average values reported. The relative standard deviations of replicates were calculated for all samples and found to be <5.0%. NO₃⁻ and NH₄⁺ concentrations were measured at precisions of 2.6% and 8.6%, respectively. DTP was determined by ICP-OES (Worsfold et al., 2016) at precisions of 3.4%. Samples were analyzed at the Center for Physical and Chemical Analysis of the Institute of Geographic Sciences and Natural Resources Research (Beijing, China).

Aquatic CO₂, CH₄, and N₂O concentrations were measured in duplicate using the headspace method. 100 mL headspace was created with ambient air in a 250 mL glass reagent bottle filled with bubble-free water. Headspace gas samples were then transferred to gas bag by a syringe and transported to our lab for measurement. We analyzed our samples using cavity ring-down spectroscopy (CRDS) (Picarro-G2508, Picarro, USA). Certified calibration gases of 300, 600, and 1000 ppm CO₂ in N₂ were used for calibration. For CH₄ and N₂O, we used the purified N₂ (99.99%) for zeroing check. The replicate measurements were within 6% of the accepted standard for all three gases. The CO₂, CH₄, and N₂O concentrations were measured at precisions of 300 ppb, 7 ppb, and 10 ppb, respectively. The detection limits of CRDS technology were reported by Brannon et al. (2016) using minimum detectable slopes. The original GHG concentrations were then calculated according to the headspace ratio and equilibration temperature, respectively. We corrected CO₂ headspace results using measured alkalinity considering chemical equilibration of the carbonate system in the sample vials (Koschorreck et al., 2021) (details in SI Text S1).

2.3. Hydrology and geography delineation

Discharge (Q) data for the study period were collected from the Water Resources Monitoring Report released by the Yangtze River Conservancy Commission in October and November of 2021. Elevation of the sampling sites was recorded with GPS during sampling. We delineated the basin boundary using the HydroATLAS data (Linke et al., 2019). Sub-basins at level of 7 were extracted to determine the variations of land covers along the Yangtze River. For the analyses of percentages of land covers, we used the land cover information provided by the dataset of Copernicus Global Land Service in 2019 (<https://land.copernicus.eu/global/products/lc>). Land cover in our study area was classified into forest, shrubs, herbaceous vegetation, cropland, urban/built-up (referred to as “urban” hereafter), bare/sparse vegetation, inland water bodies, and herbaceous wetland (referred to as “wetland” hereafter). The geodata maps were generated using QGIS 3.18 (QGIS Development Team, 2021).

2.4. Statistical techniques

We firstly considered the spatial variability among upstream, midstream, and downstream by applying analysis of covariance (ANOVA). To analyze the relationship between CO₂ and O₂ saturation, we calculated the excess saturation calculated from Henry's law corrected for temperature with the *rMR* package (Moulton, 2018).

To assess whether the available set of variables offers reasonable predictions of GHGs, we calculated linear correlations of GHG concentrations with water physiochemical variables as well as hydromorphological factors in the mainstream samples. The generated predictors of GHG concentrations had significant multicollinearity (Figure S1) and such multicollinearity violates a key assumption of multiple regression models. Stepwise linear regressions were performed to identify key explanatory variables. Stepwise regressions can reduce the number of predictors to generate the most parsimonious linear regression models and avoid the effects of multicollinearity on model results. Log-transformation was applied to the data to fulfill the requirement of normalized distribution.

In natural systems, input predictors and outcome response are often nonlinearly correlated and predictors interact with each other, resulting

in weak explanation by simple linear regression. To understand whether the potential nonlinear model can improve our ability to predict GHGs over linear regression in the Yangtze River, regression tree analysis of GHGs was performed with the *rpart* package (Therneau et al., 2019). Regression tree, as a non-linear regression method, is able to explore the original data without prior assumption. Regression tree uses a tree-like graph to map the observed predictor data to draw conclusions about the target response value. The model iteratively divides data into two subgroups based on a threshold, which distinctly makes two subgroups as different as possible by minimizing the variation (sum of squares) of the response variable within two groups (De'ath and Fabricius, 2000). We applied a 10-fold cross-validation procedure to evaluate the performance on the datasets. The most parsimonious regression tree was selected by pruning the tree when a split happens only if it decreases the error metric by a cost complexity factor of 0.001. We report the percent variation (R square) which was calculated as 1 minus the relative error (Venkiteswaran et al., 2014) to describe the fit of the tree. All statistical analyses were performed with R version 3.14.0 (R Core Team, 2021). The data that support the findings of this study are available from the corresponding author upon request.

3. Results

3.1. River characteristics

The datasets contain a large range of flow distance (the distance from estuary, 0–2576 km) and elevations (0–261 m, Fig. 1). Land covers changed remarkably with more urban land and less forest towards downstream. Most sub-catchments have more than 40% of cropland. The midstream reach had more wetlands than the other reaches (Table 1).

Water temperature during the sampling period averaged 19.4°C with very limited variation (18.8–20.1 °C). Specific conductivity ranged from 239 $\mu\text{S cm}^{-1}$ in the lower reach (corresponding to high discharge) to 407 $\mu\text{S cm}^{-1}$ in the upper reach (corresponding to low discharge). 85% of observations were undersaturated in O_2 (overall range: 6.65–9.51 mg L^{-1} , i.e., 76–105% of the saturation level). O_2 , NO_3^- , and DTP concentrations have significant differences among three river reaches (Fig. 2) with higher values in the lower reach of Yangtze River. Due to relatively

constant water temperature, no significant correlation between water temperature and other water chemical parameters was found (Figure S1).

3.2. GHGs and the spatial extent in the Yangtze River and its tributaries

We observed consistent supersaturation of three GHGs with respect to the atmosphere. Consequently, the river was net sources of GHGs. The median concentrations of dissolved CO_2 , CH_4 , and N_2O were 67 $\mu\text{mol L}^{-1}$, 0.25 $\mu\text{mol L}^{-1}$, and 59 nmol L^{-1} , respectively. CO_2 and N_2O varied among different river sections with higher values in the middle reach. CO_2 and N_2O shared similar spatial distributions, such that upper and lower reaches had significant difference from the middle reach while there was no significant difference between the upper and lower reaches (Fig. 3). For CO_2 and N_2O , the highest variability was found in the middle reaches. In contrast, CH_4 variability was not significantly different between river reaches. Compared to the mainstem, tributaries had higher GHG concentrations, which fluctuated in a wider range (Fig. 3, Table S1).

3.3. Predictability of GHGs

No significant correlations emerged between river lengths and GHG concentrations (ANOVA, $p > 0.3$ for all gases, Table S2). However, the flow significantly predicted CO_2 and N_2O at our sampling sites. Wetland and urban land among all land covers affected CO_2 and N_2O with higher CO_2 and N_2O concentrations in sub-catchments that had higher percentages of wetland and urban areas. O_2 , NO_3^- , and DTP were negatively correlated to CO_2 and N_2O . Compared to CO_2 and N_2O , we only found EC and DTP as explanatory variables for CH_4 with weak explanatory power. CO_2 and O_2 saturation varied considerably among different river sites. All mainstream samples varied between over- and under-saturation of O_2 with constant CO_2 supersaturation. The river showed an offset relative to the 1:1 line (Fig. 2), indicating that there was an external source of CO_2 uncoupled from O_2 .

In the regression tree model, the percentage of wetland coverage (wetland%) was identified as the strongest predictor of CO_2 as wetland was the first and primary branch. The tree has higher explanatory power ($R^2 = 0.49$, Fig. 4a) compared to stepwise linear regression with O_2 ,

Table 1

Characteristics of the geographic characteristics, catchment landcover, and water physical and chemical information among the upper reach, middle reach, and lower reach of the mainstem of Yangtze River ($n = 76$). The statistic information is shown as median values with the interquartile range in parentheses.

Variable	Abbr.	Unit	Upper	Middle	Lower
River characterization					
River length	Length	km	2187 (2055–2379)	1087 (875–1381)	42 (0–144)
Number of Sampling			32	26	18
Elevation	Ele	m	175 (158–215)	24 (19–33)	0 (0–3)
Discharge	Q	$10^3 \text{ m}^3 \text{ s}^{-1}$	9.7 (7.9–12.8)	26.3 (22.2–30.4)	29.6 (29.6–29.7)
Catchment landcover					
Wetland	–	%	0.8 (0.5–1.4)	5.3 (2.5–6.8)	3.7 (3.3–4.3)
Cropland	–	%	42.5 (40.2–54.5)	50.7 (38.8–63.5)	44.8 (42.5–47.1)
Urban	–	%	3.9 (2.1–12.2)	9.9 (7.2–10.8)	37.3 (25.6–37.3)
Forest	–	%	41.8 (33.1–51.2)	20.5 (7.9–33.6)	6.7 (6.7–16.2)
Water chemical and physical parameters					
Water temperature	WT	°C	19.3 (18.9–19.6)	20.3 (19.8–20.9)	18.6 (18.2–19.3)
Specific conductivity	EC	$\mu\text{S cm}^{-1}$	356 (351–364)	346 (339–360)	306 (296–318)
pH		Unitless	7.9 (7.8–7.9)	7.7 (7.6–7.8)	7.8 (7.6–7.8)
Dissolved oxygen	O_2	mg L^{-1}	8.6 (8.5–8.7)	8.7 (8.4–8.8)	8.9 (8.8–9.2)
Alkalinity	Alk	mmol L^{-1}	1.20 (1.10–1.21)	1.20 (1.13–1.30)	1.00 (1.00–1.01)
Ammonium	NH_4^+	mg L^{-1}	0.03 (0.01–0.07)	0.11 (0.07–0.14)	0.05 (0.04–0.09)
Nitrate	NO_3^-	mg L^{-1}	6.0 (5.4–6.6)	5.7 (4.5–8.7)	7.4 (7.0–7.7)
Dissolved total phosphorous	DTP	$\mu\text{g L}^{-1}$	21.2 (14.2–32.4)	12.7 (7.4–16.4)	86.1 (74.2–93.3)
Carbon dioxide	CO_2	$\mu\text{mol L}^{-1}$	67 (57–72)	87 (79–101)	69 (65–73)
Methane	CH_4	$\mu\text{mol L}^{-1}$	0.26 (0.23–0.39)	0.21 (0.19–0.32)	0.37 (0.18–0.53)
Nitrous oxide	N_2O	nmol L^{-1}	53 (49–58)	75 (68–84)	58 (55–60)

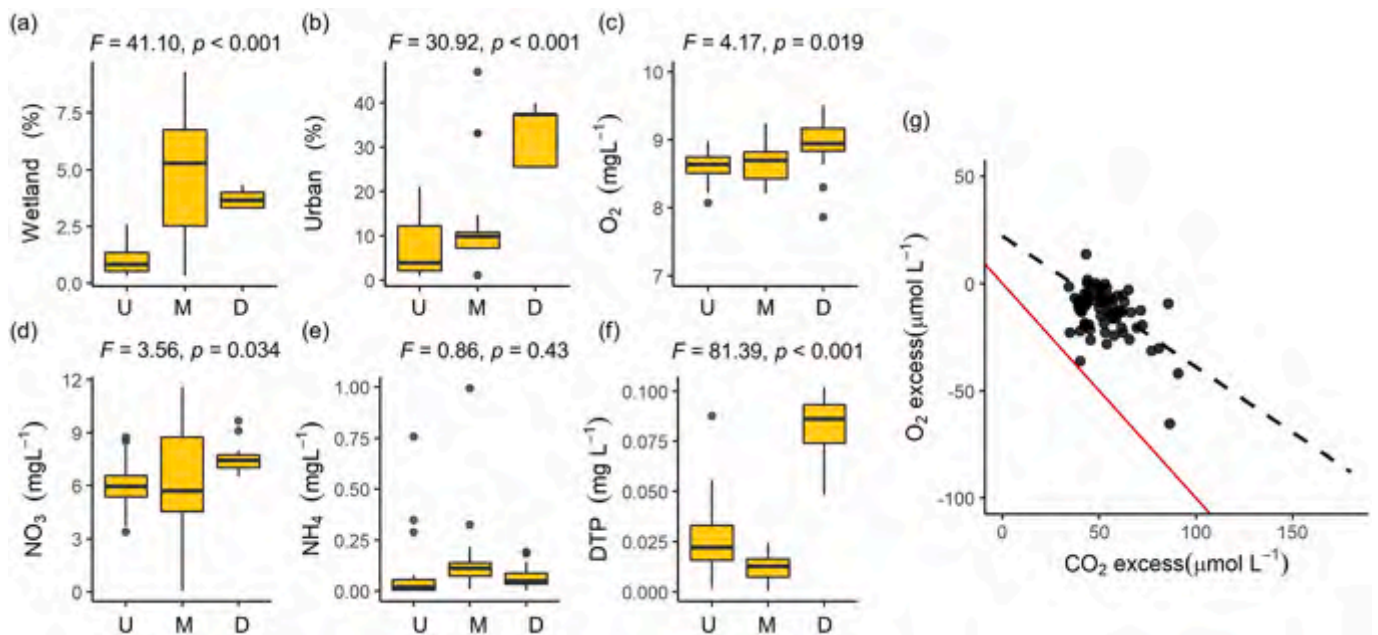


Fig. 2. Boxplot of (a) the percentage of wetland, (b) the percentage of urban land, (c) dissolved oxygen (O_2) concentrations, (d) nitrate (NO_3^-) concentrations, (e) ammonium (NH_4^+) concentrations, and (f) dissolved total phosphorous (DTP) concentrations in the mainstem of Yangtze River classified by upper reach (U), middle reach (M), and lower reach (L), respectively. The box represents the first and third quartile, the horizontal line corresponds to the median. The ANOVA (analysis of variance) results were denoted to show the significant differences of the three mainstem reaches. (g) Relationship between dissolved CO_2 and O_2 . Excess CO_2 or O_2 was calculated as the difference between measured concentrations and equilibrium concentrations expected if the stream water was in equilibrium with the atmosphere (100% saturation). The dashed 1:1 line represents the expected relationship between O_2 and CO_2 under the assumption that aerobic metabolism accounts for the measured CO_2 concentrations. The black dashed line represents the linear regression between O_2 and CO_2 across sites ($R^2 = 0.37$, $p < 0.0001$).

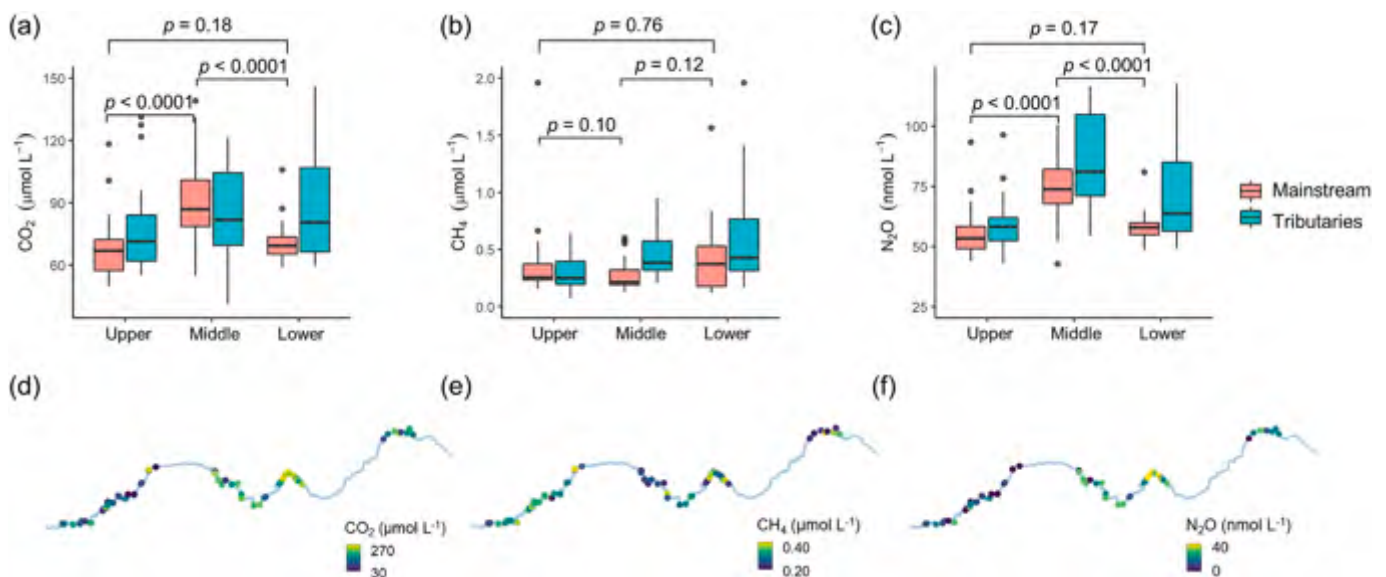


Fig. 3. (a-c) Boxplots of carbon dioxide (CO_2), methane (CH_4), and nitrous oxide (N_2O) in molar concentrations in the mainstem and tributaries of the Yangtze River classified by upper reach, middle reach, and lower reach in October–November 2020, respectively. The box represents the first and third quartile, the horizontal line corresponds to the median. The ANOVA (analysis of variance) results were denoted to show the significant differences of the three mainstem reaches. (d-f) Map of concentrations of CO_2 , CH_4 , and N_2O observed in the mainstem of Yangtze River, respectively.

NO_3^- , and wetland as predictors ($R^2 = 0.32$, $p < 0.001$, Table S3). Extremely high CO_2 concentrations occurred when wetland% exceeded 5.9%, where sampling sites were mostly distributed in the middle reach. Wetland% entered the regression tree a second time, predicting higher CO_2 concentration at more than 2.2% of wetland percentage. Low wetland% and low O_2 had the lowest CO_2 concentrations.

CH_4 concentrations were moderately predicted by O_2 and CO_2 ($R^2 = 0.31$, Fig. 4b). O_2 explains much of the variability in CH_4 , which was

high when $O_2 < 8.3 \text{ mg L}^{-1}$. Above 8.3 mg L^{-1} of O_2 , CH_4 could be further split by CO_2 ($98 \text{ } \mu\text{mol L}^{-1}$) in the tree regression model. High CH_4 was correlated with combination of lower O_2 ($< 8.3 \text{ mg L}^{-1}$) and higher CO_2 ($\geq 98 \text{ } \mu\text{mol L}^{-1}$). Regression tree analysis improved the explanatory power compared to the multiple linear regression ($R^2 = 0.19$, $p < 0.001$, Table S3).

CO_2 and DTP were chosen as predictors of N_2O concentrations in the regression tree model, which could explain 68% of the total variation

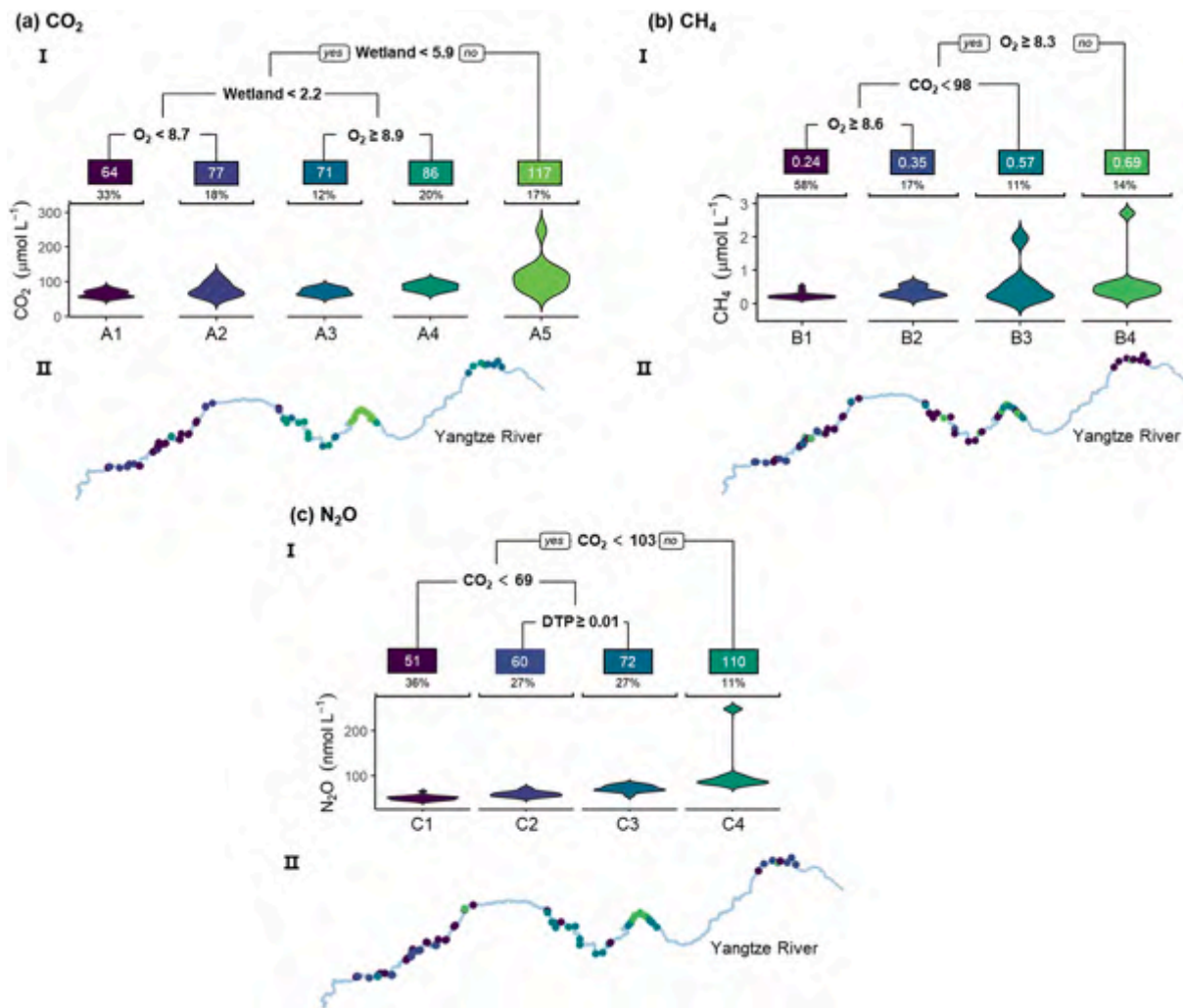


Fig. 4. Groups of sampling sites illustrating the relationships among parameters predicting GHG concentrations in the mainstem of Yangtze River. (I) Regression tree of predictors influencing GHG concentrations. Parameters entering the models were the percentage of wetland in watershed (wetland, %), dissolved oxygen (O_2 , $mg L^{-1}$), dissolved total phosphorous (DTP, $mg L^{-1}$), and carbon dioxide (CO_2 , $\mu mol L^{-1}$). Values at the end of each terminal node indicate the mean concentrations of CO_2 ($\mu mol L^{-1}$), CH_4 ($\mu mol L^{-1}$), and N_2O ($nmol L^{-1}$) with the percentage of observations below. Letters refer to the different terminal nodes (groups), where the density and spatial distribution about each group about is provided below. Violin plots under each terminal node show the median and distribution of the GHG concentrations within each regression tree leaf. (II) Spatial representation of sampling sites within each terminal node, showing that sampling sites that have similar GHG concentrations share the predictors along the Yangtze River. Cross-validated root mean squared error was 13.5, 0.13, 0.20 and R^2 was 0.49, 0.31, and 0.68 for CO_2 , CH_4 , and N_2O , respectively.

(Fig. 4c). CO_2 marked the first and second split in the regression tree, reflecting the important role of CO_2 on N_2O . Here the performance of stepwise linear model is similar to the nonlinear regression (Table S3). In linear correlations, N_2O concentrations were significantly correlated to CO_2 with high explanatory power ($R^2 = 0.59$, $p < 0.001$, Table S3).

4. Discussion

4.1. Spatial variation in GHG concentrations

The magnitudes of our measured CO_2 concentrations are comparable to previous reported annual average ranges in the Yangtze River (1235 and 1463 μatm) from Liu et al. (2016) and Ran et al. (2017), which were calculated from alkalinity and pH. Those are also at the same magnitude as for high-order rivers in the US and the global average estimate (Lauerwald et al., 2015; Liu and Raymond, 2018). Observed CH_4 and N_2O concentrations were two and three orders of magnitude lower than CO_2 , respectively. CH_4 concentrations in the mainstream were lower than the values reported by the small-scale studies at the Yangtze River Estuary (Wang et al., 2009) and Three Gorges Reservoir (Bai et al., 2022)

likely due to stronger microbial activities at reservoirs and estuaries.

Unlike other findings (Liu et al., 2016), we did not observe a continuous gradient of increase or decrease of GHGs along the Yangtze River. In contrast, CO_2 and N_2O concentrations were higher in the middle reach than in the upper and lower reaches. This is consistent with previous historical calculated CO_2 data, which did not show a longitudinal trend along the mainstem of the Yangtze River (Ran et al., 2017). Decline patterns of GHGs along rivers could be due to lower relative land–water connection than a large volume of the downstream reach (Crawford et al., 2013; Hotchkiss et al., 2015). Higher CO_2 and N_2O , in fact, are significantly linked to larger wetland coverage in the sub-catchments of the middle reach of the Yangtze River (Fig. 4). The finding is in concert with many studies, which concluded that riparian wetland is one of the major contributors of riverine GHGs (Borges et al., 2019; Leng et al., 2021; Mwanake et al., 2019; Teodoru et al., 2015).

Gases from the upstream would have a limited effect on the downstream reach because GHG outgassing is usually fast compared to downstream transport (Crawford et al., 2014). According to the gas transfer coefficient (averaged k_{600} from chamber measurements of 9.1 $m d^{-1}$, Liu et al. (2017)) and channel hydraulic geometry (averaged river

depth of 5.2 m, averaged flow velocity of 1.71 m s^{-1}) in the Yangtze River, $\sim 95\%$ of CO_2 in a given parcel of water would outgas within 84 km downstream. With longer water residence time, aquatic CH_4 can be oxidized by methanotrophic bacteria, leading to less CH_4 downstream. In large rivers, the rapidly overturned water transport limited CH_4 downstream due to outgassing and CH_4 oxidation (Sawakuchi et al., 2016). Compared to other gases, CH_4 varied without clear large-scale spatial patterns. It is likely that CH_4 is majorly derived from point sources that were subjected to strong localized control. Variance in CH_4 at smaller spatial scales therefore may overwhelm any larger scale pattern (Crawford et al., 2014). Accordingly, we could also infer that TGD is likely not the cause of higher GHGs in the middle reach since the effect of TGD can hardly be detected from the sites in the middle reach, which are 40–790 km downstream (Figure S2).

4.2. Controls of spatial pattern of GHGs

Our results on GHGs concentrations from regression trees imply both nonlinear effects and complex interactions among variables. In our case, GHGs were better predicted using nonlinear regression trees than linear regressions (Fig. 4 and Table S3), suggesting the non-linear model is capable of improving the predictive ability of the GHG concentrations. Land cover and dissolved oxygen appear to be key factors influencing spatial trends of dissolved GHGs in the Yangtze River.

The regression tree of CO_2 concentrations shows that the prediction of CO_2 relies on the combination of wetland coverage and O_2 . High wetland coverage was clearly associated with highest CO_2 , which suggests that direct or indirect inputs of CO_2 from adjacent wetland probably support a large part of riverine CO_2 (Abril et al., 2013). Good hydrologic connectivity of wetland therefore facilitates the contribution from terrestrial inputs. During our sampling period, the discharge was ~ 1.25 times higher than the annual average discharge. Thus, we assume that the river channel was well connected to riparian wetlands. This is also supported by the positive correlation between CO_2 and discharge, indicating high discharge promotes the inputs of GHGs. Although many studies have shown that agricultural land significantly contributes to aquatic GHGs due to elevated organic matter, nutrients, and sediments (Borges et al., 2018; Crawford et al., 2017b; Peacock et al., 2019; Romeijn et al., 2019), we did not observe the effect of agricultural land use on riverine GHGs. It is likely due to relatively constant agricultural land use along the river (Table 1). Given the evidence that urban land was positively correlated to GHGs, we speculate that urban land contributes to riverine GHGs via increasing inputs from point sources (NO_3^- and DTP) (Figure S1). Previous studies suggest urban rivers have 2–4 times higher CO_2 fluxes and can be CH_4 hotspots due to elevated sedimentation and nutrients (Wang et al., 2018; Wang et al., 2017; Zhang et al., 2021).

Oversaturated CO_2 in the Yangtze River is sustained by not only external, but also internal sources. The negative relationships between CO_2 and O_2 in the linear correlation analysis suggest control of riverine GHGs by metabolic linkage. Previous study found similar correlations, which were primarily attributed to heterotrophic respiration of river organic carbon as an essential CO_2 contributor (Liu et al., 2016). It should be noted, however, that the correlations do not necessarily imply in-stream metabolic activity, as external input derived from terrestrial soil respiration or groundwater can also provide the signal of low O_2 and high CO_2 (Bernal et al., 2022). While due to rapid gas exchange and modest contribution relative to huge river discharge, the input from groundwater can rarely shape the CO_2 - O_2 correlations in large rivers independent of in-stream metabolism (Liu et al., 2021; Vachon et al., 2020). The contributions of internal production to riverine CO_2 varied among different studies. Liu et al. (2016) stated that heterotrophic respiration constitutes 8–22% of excess pCO_2 in the Yangtze River. Riverine internal respiration has been shown to account for $\sim 39\%$ of the CO_2 emissions in large rivers of United States (Hotchkiss et al., 2015). The strong negative relationship between O_2 and CO_2 is indicative of the

interaction between respiration and primary production that may occur in water column and adjacent wetland (Fig. 4) (Borges et al., 2015b; Hotchkiss et al., 2015). The molar ratio (~ 1.2) shown in Fig. 2 represents the expected relationship between O_2 and CO_2 when aerobic reaction is responsible for much of the spatial variability in CO_2 concentrations. Our data generally fall to the right of this 1:1 line, implying that there are additional sources of CO_2 beyond aerobic respiration. This decoupling between CO_2 and O_2 can be attributed to (1) the external CO_2 sources (i.e. groundwater input and riparian wetland respiration) (Bernal et al., 2022), (2) anaerobic processes (for example, denitrification and methanogenesis may also contribute to additional production of CO_2) (Aho et al., 2021; Chen et al., 2015; Crawford et al., 2014; Herreid et al., 2021), and (3) carbonate buffering by conversion toward CO_2 from ionized forms (HCO_3^- and CO_3^{2-}) (Stets et al., 2017). Our results show that O_2 , as a proxy of carbon processing and transporting, is well representing CO_2 dynamics in rivers (Stets et al., 2017).

CH_4 concentrations were surprisingly poorly predicted by water chemical variables and land covers. Even though CH_4 was able to be split by O_2 and CO_2 in the regression tree analysis (Fig. 4b), these proxies of internal production and external inputs had weak explanatory power, suggesting a complex combination of factors governing CH_4 . However, all the interactions between O_2 and CO_2 in the nonlinear model (Fig. 4b) point to the conditions of ecosystem respiration (ER) as a determinant of CH_4 in the Yangtze River. The conditions that determine overall ER (including CO_2 production) also determine CH_4 production (Stanley et al., 2016). Another explanation for the unclear large-scale spatial pattern is that fluctuation in CH_4 concentrations can be subjected to strong localized control (Leng et al., 2021). Bussmann et al. (2022) highlighted that river morphology and structures determine the variability of dissolved CH_4 in large rivers. Besides this, our data showed CH_4 had no relationship with CO_2 or N_2O . Positive correlations between CO_2 and CH_4 would indicate both gases are largely controlled by organic matter degradation (Zhang et al., 2021). Positive correlation between CH_4 and N_2O was observed due to large inputs of untreated human waste (Zhang et al., 2021). Further, negative correlation between both was reported in Smith and Böhlke (2019) because both gases respond differently to biogeochemical controls (different response to NO_3^-). Our results are perhaps not surprising as the contribution of anaerobic metabolism and biogeochemical controls shifts over space and time. CO_2 derived from metabolism might probably happen in water column and surrounding wetland, while CH_4 production might be supported by fine organic matter-rich sediments (Wilcock and Sorrell, 2008). Nutrient enrichment can change the relative contributions of different respiratory pathways within fluvial systems, as well as net GHG emissions, resulting in unclear ratios among three gases (Stanley et al., 2016).

Interestingly, we found N_2O concentrations were most strongly predicted by CO_2 in the mainstem of the Yangtze River, explaining 59% of its variation (Table S2). Our positive relationship between CO_2 and N_2O is in accordance with Laini et al. (2011) in lowland springs, Leng et al. (2022) in the river network of the North China Plain, and Venkiteswaran et al. (2014) in agricultural streams, but opposite to other studies that concluded with negative correlations (Teodoru et al., 2015). The negative correlations were resulted from N_2O removed by denitrification, which was intensified by organic matter degradation in the sediments, simultaneously producing CO_2 (Teodoru et al., 2015). We infer our positive correlation between N_2O and CO_2 is mainly due to processes favored by similar environmental conditions, rather than the direct dependence of N_2O on CO_2 . The strong correlation of both gases is possibly the consequence of simultaneous transportation, production, and consumption of both gases. Both gases share common environmental predictors with similar explanatory power (e.g., O_2 , wetland, discharge in Table S2). Spatial patterns of CO_2 and N_2O in rivers are believed to be attributed to the connectivity with wetlands (Borges et al., 2019). One of the evidences is the dominance of wetlands in N_2O variations when CO_2 is excluded from the predictors of N_2O , indicating

wetlands are playing a significant role in regulating riverine N_2O (Table S4). In addition to the wetland inputs, the production of N_2O , as the same as CO_2 , occurs in the hyporheic zone along groundwater flow paths and in the water column where O_2 is low (Mwanake et al., 2019; Yang and Lei, 2018). Respiration, particularly at locations that receive large amounts of organic matter, may deplete O_2 and produce CO_2 , facilitating denitrification in the hyporheic zone and contributing to the accumulation of excess GHGs in the water column. Similar relationships between CO_2 and N_2O were observed in Mwanake et al. (2019) and Dai et al. (2008), being explained by nitrification via ammonium oxidizing bacteria producing CO_2 through H^+ production. It is reasonable that both nitrification and denitrification are contributing to N_2O production through a coupled nitrification–denitrification process, which is favorable under suboxic conditions (Wrage et al., 2001). In this process, denitrifiers reduced NO_3^- produced by aerobic nitrification, leading to N_2O production (Maavara et al., 2019; Quick et al., 2019). In addition, the optimum for a net N_2O production by nitrification, nitrifier denitrification, and denitrification lies between a pH of 7–7.5 (Blum et al., 2018), implying the net N_2O production could be moderate in the river because of higher pH in our system (Table 1).

We speculate there is no N limitation in our systems. Dissolved inorganic nitrogen (NO_3^- and NH_4^+) was at high levels comparable to some agricultural rivers (Borges et al., 2018). That could be the explanation for our weak negative correlation between N_2O and NO_3^- , which is opposite to a series of studies that reported strong positive relationships between N_2O and NO_3^- (Beaulieu et al., 2011; Turner et al., 2016). Previous studies reported that N_2O flux (Turner et al., 2016) or yield (Silvennoinen et al., 2008) increased with nitrate up to a certain point, and then leveled off. Insignificant relationship between NO_3^- and N_2O was also observed in 9 of 12 African river (Borges et al., 2015b) and nitrogen-enriched rivers in the Chaohu Lake Basin (Yang and Lei, 2018). Of note is that the model proposed by Intergovernmental Panel on Climate Change (IPCC), which predicts riverine N_2O flux by NO_3^- with a single linear function is not sufficient. The equation derived from average $\text{NO}_3^-/\text{N}_2\text{O}$ ratios (default value of 0.0025) in shallow groundwater is widely applied to estimate the riverine N_2O flux (Nevison, 2000; Syakila and Kroeze, 2011). Thus, we argue that the linear equation from the IPCC methodology to estimate riverine N_2O needs to be applied with caution (Maavara et al., 2019; Venkiteswaran et al., 2014; Webb et al., 2021). We recommend an improvement of the IPCC model by using a saturation model, instead of flux model as the gas transfer process is not included.

Apart from terrestrial inputs and in-stream processing, we considered TGD and tributaries had little effect on spatial patterns of GHGs in the mainstem of the Yangtze River. We have demonstrated that outgassing is a rapid process, resulting in a profound effect limited to the vicinity of the reservoir (Figure S2). Another evidence for the minor influence of the dam is the low relative importance of dam (6–28%, Table S4) on spatial variations of GHGs compared to other predictors (wetlands and O_2) from the results of nonlinear regressions. Ni et al. (2022) reported the longitudinal variation before and after TGR with a finer spatial resolution, where the GHG concentrations were increased by the reservoir itself and decreased by habitat modification downstream of the dam within tens of kilometers. Our closest sampling site downstream of TGD is 35 km away, therefore TGD might have little impact from there on. As a result, the net change in GHG emissions directly caused by the TGR is unable to alter the overall GHG trends from the perspective of the entire Yangtze River. The dam has altered the riverine habitats downstream, leading to essential changes in river topology and biogeochemical cycles. The floodplain erosion is most potent after the Three Gorges Dam and declines gradually downstream (Sun et al., 2020). As a result, the large wetland coverage in the middle reach could be an indirect effect of damming. Consequently, the effect of damming on GHGs can be masked behind the information from wetland coverages. The budgets of dissolved GHGs from tributaries were generally much lower than the budget of GHGs in the mainstem

(Bussmann et al., 2022). We modeled GHG budgets at the inflow of tributaries, upstream and downstream across different river sections assuming conservative mixing (Text S2), and found the expected dilution of tributaries was lower than the measured budgets downstream (Figure S3 and Table S5). It suggests that GHG import from tributaries is insufficient to remarkably affect the mainstream. Even though GHG concentrations in tributaries were higher, considering lower relative discharge of the tributaries than that of the Yangtze River, tributaries only marginally affect the GHG concentrations. The minor effect of tributaries to dissolved GHGs can also apply to other point sources with low-volume high-GHG inputs. It also explains the unclear large-scale pattern of CH_4 since CH_4 is mostly locally controlled.

5. Conclusions and implications

Our study provides the first systematic estimate of the longitudinal variability of greenhouse gases (GHGs) along the Yangtze River and land cover and water biogeochemical impacts on three GHGs. There are no continuous longitudinal gradients for GHGs. The spatial trend of CO_2 was similar to that of N_2O , with higher values in the middle reach of Yangtze River. Regression tree approach improves explanatory power over simple linear regression, and is a step towards better integration and understanding of environmental predictors of riverine GHGs. Our results show that wetland and O_2 drive the responses of CO_2 and CH_4 , meanwhile, CO_2 is the best predictor of N_2O concentration in the system, which underscores the importance of identifying the correlations between GHGs and understanding the nature of such correlations for future prediction of GHGs. We demonstrate that instead of the direct effect of Three Gorges Dam and tributaries, terrestrial influence and in-stream metabolization dominate the spatial variations of GHGs.

The Yangtze River is currently confronted by increase in precipitation and temperature (Birkinshaw et al., 2017), with increased discharge and mobilization of OC in soils (Li et al., 2018). These changes are altering the functioning of riverine ecosystems and appearing to have larger contribution of wetland ecosystem on CO_2 and N_2O suggested by our study. As suggested by Richey et al. (2002) that river and floodplain waters in the Amazon basin maintain high CO_2 and constitute an important carbon loss, we recommend to include wetland contribution in riverine GHG budgets and its response to environmental change (eutrophication, droughts, etc.) for the estimates of riverine GHGs. The Yangtze River can play an important role of CH_4 processes with more terrestrial inputs of organic carbon, while the relationship between water temperature and CH_4 concentration in streams and rivers is ambiguous (Stanley et al., 2016). Thus, three gases may respond uniquely to global change, and the variability needs to be captured in future studies. By reduction of direct organic and nutrient inputs from wastewater treatment plants and farming management, controlling eutrophication, which is the key factor in regulating the organic matter cycling in the Yangtze floodplain lakes (Zeng et al., 2022), can help decrease aquatic CH_4 and N_2O emissions in such human-dominated landscapes.

We acknowledge that our results are biased toward high flow conditions, which may lead to an overestimation of dissolved GHG concentrations. In the future, repeated measurements over time (time scale ranging from sub-daily to seasonal) are necessary to elucidate how spatial patterns in fluvial systems change. It is a challenge to match the scales of observations to the scales of the drivers of GHG emissions. The Yangtze River is large and diverse, with variations in C export and metabolism. As such, further detailed investigations on internal metabolism and gas transfer measurement are needed to capture the variability of multiple processes to obtain a more holistic understanding of GHG emissions in this important large river system. We recommend to carefully account for the contribution of GHG emissions from large river systems considering the importance of large river feedback on climate change and the linkage of catchment land–atmosphere and land–ocean carbon exchange.

CRedit authorship contribution statement

Peifang Leng: Conceptualization, Methodology, Visualization, Writing – original draft, Writing – review & editing. **Zhao Li:** Data curation, Investigation, Methodology. **Qiuying Zhang:** Conceptualization, Funding acquisition. **Matthias Koschorreck:** Supervision, Writing – review & editing. **Fadong Li:** Resources, Supervision, Writing – review & editing. **Yunfeng Qiao:** Data curation, Resources. **Jun Xia:** Funding acquisition, Project administration.

Declaration of Competing Interest

The authors declare that they have no known competing financial interests or personal relationships that could have appeared to influence the work reported in this paper.

Data availability

Data will be made available on request.

Acknowledgements

This study was supported by the Major Program of the National Natural Science Foundation of China (No. 41890823 and No. U1906219). P. Leng is supported by the CSC-DAAD Joint Fellowship Programme for postdoctoral research and China Postdoctoral Science Foundation under Grant No. 2022M723122. Thanks to Jianqi Wang, Kai Fu, and Yu Peng for sample analysis and colleagues at the Helmholtz Centre for Environmental Research-UFZ for valuable discussions. We thank Prof. Gang Chen for language check. The authors declare no competing interests. The datasets used and analyzed in this study are available from the corresponding author on reasonable request.

Appendix A. Supplementary data

Supplementary data to this article can be found online at <https://doi.org/10.1016/j.jhydrol.2023.129710>.

References

- Abril, G., Martinez, J.-M., Artigas, L.F., Moreira-Turcq, P., Benedetti, M.F., Vidal, L., Meziane, T., Kim, J.-H., Bernardes, M.C., Savoye, N., Deborde, J., Souza, E.L., Albric, P., Landim de Souza, M.F., Roland, F., 2013. Amazon River carbon dioxide outgassing fuelled by wetlands. *Nature* 505, 395.
- Aho, K.S., Fair, J.H., Hosen, J.D., Kyzivat, E.D., Logozzo, L.A., Rocher-Ros, G., Weber, L.C., Yoon, B., Raymond, P.A., 2021. Distinct concentration-discharge dynamics in temperate streams and rivers: CO₂ exhibits chemostasis while CH₄ exhibits so. *Limnol. Oceanogr.*
- Bai, X., He, Q., Li, H., Xu, Q., Cheng, C., 2022. Response of CO₂ and CH₄ transport to damming: a case study of Yulin River in the Three Gorges Reservoir, China. *Environ. Res.* 208, 112733.
- Beaulieu, J.J., Tank, J.L., Hamilton, S.K., Wollheim Jr, W.M., Mulholland, P.J., Peterson, B.J., Ashkenas, L.R., Cooper, L.W., Dahm, C.N., 2011. Nitrous oxide emission from denitrification in stream and river networks. *Proc. Natl. Acad. Sci. USA* 108 (1), 214.
- Bernal, S., Cohen, M.J., Ledesma, J.L.J., Kirk, L., Martí, E., Lupon, A., 2022. Stream metabolism sources a large fraction of carbon dioxide to the atmosphere in two hydrologically contrasting headwater streams. *Limnol. Oceanogr.* 67 (12), 2621–2634.
- Bernhardt, E.S., Savoy, P., Vlah, M.J., Appling, A.P., Koenig, L.E., Hall, R.O., Arroita, M., Blaszcak, J.R., Carter, A.M., Cohen, M., Harvey, J.W., Heffernan, J.B., Helton, A.M., Hosen, J.D., Kirk, L., McDowell, W.H., Stanley, E.H., Yackulic, C.B., Grimm, N.B., 2022. Light and flow regimes regulate the metabolism of rivers. *Proc. Natl. Acad. Sci.* 119 (8).
- Birkinshaw, S.J., Guerreiro, S.B., Nicholson, A., Liang, Q., Quinn, P., Zhang, L., He, B., Yin, J., Fowler, H.J., 2017. Climate change impacts on Yangtze River discharge at the Three Gorges Dam. *Hydrol. Earth Syst. Sci.* 21 (4), 1911–1927.
- Blum, J.-M., Su, Q., Ma, Y., Valverde-Pérez, B., Domingo-Félez, C., Jensen, M.M., Smets, B.F., 2018. The pH dependency of N-converting enzymatic processes, pathways and microbes: effect on net N₂O production. *Environ. Microbiol.* 20 (5), 1623–1640.
- Borges, A.V., Abril, G., Darchambeau, F., Teodoru, C.R., Deborde, J., Vidal, L.O., Lambert, T., Bouillon, S., 2015a. Divergent biophysical controls of aquatic CO₂ and CH₄ in the World's two largest rivers. *Sci. Rep.* 5 (15614).
- Borges, A.V., Darchambeau, F., Teodoru, C.R., Marwick, T.R., Tamooh, F., Geeraert, N., Omengo, F.O., Guerin, F., Lambert, T., Morana, C., Okuku, E., Bouillon, S., 2015b. Globally significant greenhouse-gas emissions from African inland waters. *Nat. Geosci.* 8 (8), 637–642.
- Borges, A.V., Darchambeau, F., Lambert, T., Bouillon, S., Morana, C., Brouyère, S., Hakoun, V., Jurado, A., Tseng, H.C., Descy, J.P., Roland, F.A.E., 2018. Effects of agricultural land use on fluvial carbon dioxide, methane and nitrous oxide concentrations in a large European river, the Meuse (Belgium). *Sci. Total Environ.* 610–611, 342–355.
- Borges, A.V., Darchambeau, F., Lambert, T., Morana, C., Allen, G.H., Tambwe, E., Toengah Sembaito, A., Mambo, T., Nlandu Wabakhangazi, J., Descy, J.P., Teodoru, C.R., Bouillon, S., 2019. Variations in dissolved greenhouse gases (CO₂, CH₄, N₂O) in the Congo River network overwhelmingly driven by fluvial-wetland connectivity. *Biogeosciences* 16 (19), 3801–3834.
- Brannon, E.Q., Moseman-Valtierra, S.M., Rella, C.W., Martin, R.M., Chen, X., Tang, J., 2016. Evaluation of laser-based spectrometers for greenhouse gas flux measurements in coastal marshes. *Limnol. Oceanogr.: Methods* 14 (7), 466–476.
- Bussmann, I., Koedel, U., Schütze, C., Kamjunke, N., Koschorreck, M., 2022. Spatial variability and hotspots of methane concentrations in a large temperate river. *Front. Environ. Sci.* 10, 833936.
- Chen, N., Wu, J., Zhou, X., Chen, Z., Lu, T., 2015. Riverine N₂O production, emissions and export from a region dominated by agriculture in Southeast Asia (Jiulong River). *Agric. Ecosyst. Environ.* 208, 37–47.
- Cole, J.J., Prairie, Y.T., Caraco, N.F., McDowell, W.H., Tranvik, L.J., Striegl, R.G., Duarte, C.M., Kortelainen, P., Downing, J.A., Middelburg, J.J., Melack, J., 2007. Plumbing the global carbon cycle: integrating inland waters into the terrestrial carbon budget. *Ecosystems* 10 (1), 172–185.
- Crawford, J.T., Striegl, R.G., Wickland, K.P., Dornblaser, M.M., Stanley, E.H., 2013. Emissions of carbon dioxide and methane from a headwater stream network of interior Alaska. *J. Geophys. Res.: Biogeosci.* 118 (2), 482–494.
- Crawford, J.T., Lottig, N.R., Stanley, E.H., Walker, J.F., Hanson, P.C., Finlay, J.C., Striegl, R.G., 2014. CO₂ and CH₄ emissions from streams in a lake-rich landscape: patterns, controls, and regional significance. *Glob. Biogeochem. Cycles* 28 (3), 197–210.
- Crawford, J.T., Loken, L.C., Stanley, E.H., Stets, E.G., Dornblaser, M.M., Striegl, R.G., 2016. Basin scale controls on CO₂ and CH₄ emissions from the Upper Mississippi River. *Geophys. Res. Lett.* 43 (5), 1973–1979.
- Crawford, J.T., Loken, L.C., West, W.E., Crary, B., Spawn, S.A., Gubbins, N., Jones, S.E., Striegl, R.G., Stanley, E.H., 2017a. Spatial heterogeneity of within-stream methane concentrations. *J. Geophys. Res.: Biogeosci.* 122 (5), 1036–1048.
- Crawford, J.T., Stanley, E.H., Dornblaser, M.M., Striegl, R.G., 2017b. CO₂ time series patterns in contrasting headwater streams of North America. *Aquat. Sci.* 79 (3), 473–486.
- Dai, M., Wang, L., Guo, X., Zhai, W., Li, Q., He, B., Kao, S.J., 2008. Nitrification and inorganic nitrogen distribution in a large perturbed river/estuarine system: the Pearl River Estuary, China. *Biogeosciences* 5 (5), 1227–1244.
- De'ath, G., Fabricius, K.E., 2000. CLASSIFICATION AND REGRESSION TREES: A POWERFUL YET SIMPLE TECHNIQUE FOR ECOLOGICAL DATA ANALYSIS. *Ecology* 81 (11), 3178–3192.
- Herreid, A.M., Wymore, A.S., Varner, R.K., Potter, J.D., McDowell, W.H., 2021. Divergent controls on stream greenhouse gas concentrations across a land-use gradient. *Ecosystems* 24, 1299–1316.
- Hotchkiss, E.R., Hall Jr, R.O., Sponseller, R.A., Butman, D., Klaminder, J., Laudon, H., Rosvall, M., Karlsson, J., 2015. Sources of and processes controlling CO₂ emissions change with the size of streams and rivers. *Nat. Geosci.* 8, 696.
- Hu, M., Chen, D., Dahlgren, R.A., 2016. Modeling nitrous oxide emission from rivers: a global assessment. *Glob. Chang. Biol.* 22 (11), 3566–3582.
- Koschorreck, M., Prairie, Y.T., Kim, J., Marcé, R., 2021. Technical note: CO₂ is not like CH₄ – limits of and corrections to the headspace method to analyse pCO₂ in fresh water. *Biogeosciences* 18 (5), 1619–1627.
- Kroeze, C., Dumont, E., Seitzinger, S.P., 2005. New estimates of global emissions of N₂O from rivers and estuaries. *Environ. Sci.* 2 (2–3), 159–165.
- Laini, A., Bartoli, M., Castaldi, S., Viaroli, P., Capri, E., Trevisan, M., 2011. Greenhouse gases (CO₂, CH₄ and N₂O) in lowland springs within an agricultural impacted watershed (Po River Plain, northern Italy). *Chem. Ecol.* 27 (2), 177–187.
- Lauerwald, R., Laruelle, G.G., Hartmann, J., Ciais, P., Regnier, P.A.G., 2015. Spatial patterns in CO₂ evasion from the global river network. *Glob. Biogeochem. Cycles* 29 (5), 534–554.
- Leng, P., Kamjunke, N., Li, F., Koschorreck, M., 2021. Temporal patterns of methane emissions from two streams with different riparian connectivity. *Journal of Geophysical Research. Biogeosciences* 126 (8).
- Leng, P., Li, Z., Zhang, Q., Li, F., Koschorreck, M., 2022. Fluvial CO₂ and CH₄ in a lowland agriculturally impacted river network: importance of local and longitudinal controls. *Environ. Pollut.* 303, 119125.
- Li, S., Ni, M., Mao, R., Bush, R.T., 2018. Riverine CO₂ supersaturation and outgassing in a subtropical monsoonal mountainous area (Three Gorges Reservoir Region) of China. *J. Hydrol.* 558, 460–469.
- Linke, S., Lehner, B., Ouellet Dallaire, C., Ariwi, J., Grill, G., Anand, M., Beames, P., Burchard-Levine, V., Maxwell, S., Moidu, H., Tan, F., Thieme, M., 2019. Global hydro-environmental sub-basin and river reach characteristics at high spatial resolution. *Sci. Data* 6 (1), 283.
- Liu, S., Lu, X.X., Xia, X., Zhang, S., Ran, L., Yang, X., Liu, T., 2016. Dynamic biogeochemical controls on river pCO₂(2) and recent changes under aggravating river impoundment: an example of the subtropical Yangtze River. *Glob. Biogeochem. Cycles* 30 (6), 880–897.

- Liu, S., Lu, X.X., Xia, X., Yang, X., Ran, L., 2017. Hydrological and geomorphological control on CO₂ outgassing from low-gradient large rivers: an example of the Yangtze River system. *J. Hydrol.* 550, 26–41.
- Liu, S., Kuhn, C., Amatulli, G., Aho, K., Butman, D.E., Allen, G.H., Lin, P., Pan, M., Yamazaki, D., Brinkerhoff, C., Gleason, C., Xia, X., Raymond, P.A., 2022. The importance of hydrology in routing terrestrial carbon to the atmosphere via global streams and rivers. *Proc. Natl. Acad. Sci.* 119 (11).
- Liu, S., Raymond, P.A., 2018. Hydrologic controls on pCO₂ and CO₂ efflux in US streams and rivers. *Limnol. Oceanogr. Lett.* 3 (6), 428–435.
- Liu, S., She, D., Gao, C., Amatulli, G., Wang, L., Lu, X., Raymond, P.A., Xia, X., 2021. Groundwater as a limited carbon dioxide source in a large river (the Yangtze River). *Sci. Total Environ.* 760, 143336.
- Maavara, T., Lauerwald, R., Laruelle, G.G., Akbarzadeh, Z., Bouskill, N.J., Van Cappellen, P., Regnier, P., 2019. Nitrous oxide emissions from inland waters: Are IPCC estimates too high? *Glob. Chang. Biol.* 25 (2), 473–488.
- Marzadri, A., Amatulli, G., Tonina, D., Bellin, A., Shen, L.Q., Allen, G.H., Raymond, P.A., 2021. Global riverine nitrous oxide emissions: the role of small streams and large rivers. *Sci. Total Environ.* 776, 145148.
- Moulton, T.L. 2018 rMR: Importing Data from Loligo Systems Software, Calculating Metabolic Rates and Critical Tensions, R package version 1.1.0.
- Mwanake, R.M., Gettel, G.M., Aho, K.S., Namwaya, D.W., Masese, F.O., Butterbach-Bahl, K., Raymond, P.A., 2019. Land use, not stream order, controls N₂O concentration and flux in the Upper Mara River Basin, Kenya. *J. Geophys. Res.-Biogeosci.* 124 (11), 3491–3506.
- Nevison, C., 2000. Review of the IPCC methodology for estimating nitrous oxide emissions associated with agricultural leaching and runoff. *Chemosphere – Glob. Change Sci.* 2 (3), 493–500.
- Ni, J., Wang, H., Ma, T., Huang, R., Ciaï, P., Li, Z., Yue, Y., Chen, J., Li, B., Wang, Y., Zheng, M., Wang, T., Borthwick, A.G.L., 2022. Three Gorges Dam: friend or foe of riverine greenhouse gases? *Natl. Sci. Rev.*
- Peacock, M., Audet, J., Jordan, S., Smeds, J., Wallin, M.B., 2019. Greenhouse gas emissions from urban ponds are driven by nutrient status and hydrology. *Ecosphere* 10 (3), e02643.
- QGIS Development Team 2021 QGIS Geographic Information System, Open Source Geospatial Foundation Project.
- Quick, A.M., Reeder, W.J., Farrell, T.B., Tonina, D., Feris, K.P., Benner, S.G., 2019. Nitrous oxide from streams and rivers: a review of primary biogeochemical pathways and environmental variables. *Earth-Sci. Rev.* 191, 224–262.
- R Core Team, 2021. A Language and Environment for Statistical Computing. R Foundation for Statistical Computing, Vienna, Austria.
- Ran, L., Lu, X.X., Liu, S., 2017. Dynamics of riverine CO₂ in the Yangtze River fluvial network and their implications for carbon evasion. *Biogeosciences* 14 (8), 2183–2198.
- Raymond, P.A., Hartmann, J., Lauerwald, R., Sobek, S., McDonald, C., Hoover, M., Butman, D., Striegl, R., Mayorga, E., Humborg, C., Kortelainen, P., Durr, H., Meybeck, M., Ciaï, P., Guth, P., 2013. Global carbon dioxide emissions from inland waters. *Nature* 503 (7476), 355–359.
- Regnier, P., Friedlingstein, P., Ciaï, P., Mackenzie, F.T., Gruber, N., Janssens, I.A., Laruelle, G.G., Lauerwald, R., Luysaert, S., Andersson, A.J., 2013. Anthropogenic perturbation of the carbon fluxes from land to ocean. *Nat. Geosci.* 6 (8), 597–607.
- Richey, J.E., Melack, J.M., Aufdenkampe, A.K., Ballester, V.M., Hess, L.L., 2002. Outgassing from Amazonian rivers and wetlands as a large tropical source of atmospheric CO₂. *Nature* 416 (6881), 617–620.
- Rivera-Monroy, V.H., Delaune, R.D., Owens, A.B., Visser, J., White, J.R., Twilley, R.R., Hernandez-Trejo, H., Benitez, J.A., 2011. In: *Treatise on Estuarine and Coastal Science*. Academic Press, Waltham, pp. 185–215.
- Romeijn, P., Comer-Warner, S.A., Ullah, S., Hannah, D.M., Krause, S., 2019. Streambed organic matter controls on carbon dioxide and methane emissions from streams. *Environ. Sci. Technol.* 53 (5), 2364–2374.
- Rovelli, L., Olde, L.A., Heppell, C.M., Binley, A., Yvon-Durocher, G., Glud, R.N., Trimmer, M., 2022. Contrasting biophysical controls on carbon dioxide and methane outgassing from streams. *J. Geophys. Res. Biogeosci.* 127 (1) e2021JG006328.
- Sawakuchi, H.O., Bastviken, D., Sawakuchi, A.O., Ward, N.D., Borges, C.D., Tsai, S.M., Richey, J.E., Ballester, M.V.R., Krusche, A.V., 2016. Oxidative mitigation of aquatic methane emissions in large Amazonian rivers. *Glob. Chang. Biol.* 22 (3), 1075–1085.
- Silvennoinen, H., Liikanen, A., Torssonen, J., Florian Stange, C., Martikainen, P.J., 2008. Denitrification and nitrous oxide effluxes in boreal, eutrophic river sediments under increasing nitrate load: a laboratory microcosm study. *Biogeochemistry* 91 (2–3), 105–116.
- Smith, R.L., Böhlke, J.K., 2019. Methane and nitrous oxide temporal and spatial variability in two midwestern USA streams containing high nitrate concentrations. *Sci. Total Environ.* 685, 574–588.
- Stanley, E.H., Casson, N.J., Christel, S.T., Crawford, J.T., Loken, L.C., Oliver, S.K., 2016. The ecology of methane in streams and rivers: patterns, controls, and global significance. *Ecol. Monogr.* 86 (2), 146–171.
- Stanley, E.H., Loken, L.C., Casson, N.J., Oliver, S.K., Sponseller, R.A., Wallin, M.B., Zhang, L., Rocher-Ros, G., 2022. GRiMeDB: The Global River Database of Methane Concentrations and Fluxes. Copernicus GmbH.
- Stets, E.G., Butman, D., McDonald, C.P., Stackpoole, S.M., DeGrandpre, M.D., Striegl, R. G., 2017. Carbonate buffering and metabolic controls on carbon dioxide in rivers. *Global Biogeochemical Cycles* 31 (4), 663–677.
- Sun, G., Lei, G., Qu, Y., Zhang, C., He, K., 2020. The operation of the three gorges dam alters wetlands in the middle and lower reaches of the Yangtze River. *Front. Environ. Sci.* 8.
- Syakila, A., Kroeze, C. 2011. The global nitrous oxide budget revisited. *Greenhouse gas measurement management* 1(1), 17–26.
- Teodoru, C.R., Nyoni, F.C., Borges, A.V., Darchambeau, F., Nyambe, I., Bouillon, S., 2015. Dynamics of greenhouse gases (CO₂, CH₄, N₂O) along the Zambezi River and major tributaries, and their importance in the riverine carbon budget. *Biogeochemistry* 12 (8), 2431–2453.
- Therneau, T., Atkinson, B., Ripley, B. 2019 rpart: Recursive Partitioning and Regression Trees.
- Turner, P.A., Griffis, T.J., Baker, J.M., Lee, X., Crawford, J.T., Loken, L.C., Venterea, R.T., 2016. Regional-scale controls on dissolved nitrous oxide in the Upper Mississippi River. *Geophys. Res. Lett.* 43 (9), 4400–4407.
- Vachon, D., Sadro, S., Bogard, M.J., Lapierre, J.F., Baulch, H.M., Rusak, J.A., Denfeld, B. A., Laas, A., Klaus, M., Karlsson, J., Weyhenmeyer, G.A., Giorgio, P.A., 2020. Paired O₂-CO₂ measurements provide emergent insights into aquatic ecosystem function. *Limnol. Oceanogr. Lett.* 5 (4), 287–294.
- Venkiteswaran, J.J., Rosamond, M.S., Schiff, S.L., 2014. Nonlinear response of riverine N₂O fluxes to oxygen and temperature. *Environ. Sci. Technol.* 48 (3), 1566–1573.
- Wang, D., Chen, Z., Sun, W., Hu, B., Xu, S., 2009. Methane and nitrous oxide concentration and emission flux of Yangtze Delta plain river net. *Sci. China Ser. B: Chem.* 52 (5), 652–661.
- Wang, X., He, Y., Yuan, X., Chen, H., Peng, C., Zhu, Q., Yue, J., Ren, H., Deng, W., Liu, H., 2017. pCO₂ and CO₂ fluxes of the metropolitan river network in relation to the urbanization of Chongqing, China. *J. Geophys. Res.-Biogeosci.* 122 (3), 470–486.
- Wang, X., He, Y., Chen, H., Yuan, X., Peng, C., Yue, J., Zhang, Q., Zhou, L., 2018. CH₄ concentrations and fluxes in a subtropical metropolitan river network: Watershed urbanization impacts and environmental controls. *Sci. Total Environ.* 622–623, 1079–1089.
- Ward, N.D., Bianchi, T.S., Sawakuchi, H.O., Gagne-Maynard, W., Cunha, A.C., Brito, D. C., Neu, V., De Matos Valerio, A., Da Silva, R., Krusche, A.V., Richey, J.E., Keil, R.G., 2016. The reactivity of plant-derived organic matter and the potential importance of priming effects along the lower Amazon River. *J. Geophys. Res.: Biogeosci.* 121 (6), 1522–1539.
- Webb, J.R., Santos, I.R., Maher, D.T., Finlay, K., 2019. The importance of aquatic carbon fluxes in net ecosystem carbon budgets: a catchment-scale review. *Ecosystems* 22 (3), 508–527.
- Webb, J.R., Clough, T.J., Quayle, W.C., 2021. A review of indirect N₂O emission factors from artificial agricultural waters. *Environ. Res. Lett.* 16 (4), 043005.
- Wilcock, R.J., Sorrell, B.K., 2008. Emissions of greenhouse gases CH₄ and N₂O from low-gradient streams in agriculturally developed catchments. *Water Air Soil Pollut.* 188 (1), 155–170.
- Worsfold, P., McKelvie, I., Monbet, P., 2016. Determination of phosphorus in natural waters: a historical review. *Analyt. Chim. Acta* 918, 8–20.
- Wrage, N., Velthof, G.L., van Beusichem, M.L., Oenema, O., 2001. Role of nitrifier denitrification in the production of nitrous oxide. *Soil Biol. Biochem.* 33 (12), 1723–1732.
- Wu, Y., Zhang, J., Liu, S.M., Zhang, Z.F., Yao, Q.Z., Hong, G.H., Cooper, L., 2007. Sources and distribution of carbon within the Yangtze River system. *Estuar. Coast. Shelf Sci.* 71 (1), 13–25.
- Yang, L., Lei, K., 2018. Effects of land use on the concentration and emission of nitrous oxide in nitrogen-enriched rivers. *Environ. Pollut.* 238, 379–388.
- Zeng, L., McGowan, S., Swann, G.E.A., Leng, M.J., Chen, X., 2022. Eutrophication has a greater influence on floodplain lake carbon cycling than dam installation across the middle Yangtze Region. *J. Hydrol.* 614, 128510.
- Zhang, Q., Chen, Y., Li, Z., Fang, G., Xiang, Y., Li, Y., Ji, H., 2020. Recent changes in water discharge in snow and glacier melt-dominated rivers in the Tianshan Mountains, Central Asia. *Remote Sens.* 12 (17), 2704.
- Zhang, W., Li, H., Xiao, Q., Li, X., 2021. Urban rivers are hotspots of riverine greenhouse gas (N₂O, CH₄, CO₂) emissions in the mixed-landscape chaohu lake basin. *Water Res.* 189, 116624.
- Zhang, G., Zhang, J., Liu, S., Ren, J., Xu, J., Zhang, F., 2008. Methane in the Changjiang (Yangtze River) Estuary and its adjacent marine area: riverine input, sediment release and atmospheric fluxes. *Biogeochemistry* 91 (1), 71–84.
- Zhao, Y., Wu, B.F., Zeng, Y., 2013. Spatial and temporal patterns of greenhouse gas emissions from Three Gorges Reservoir of China. *Biogeosciences* 10 (2), 1219–1230.